



OPEN

Bee-safe peptidomimetic acaricides achieved by comparative genomics

Vikas Jindal^{1,2,9}, Daqi Li^{1,3,9}, Leslie C. Rault⁴, Soheila Fatehi¹, Rupinder Singh¹, Moritz Mating¹, Ye Zou⁵, Ho-Leung Ng⁵, Krzysztof Kaczmarek^{6,7}, Janusz Zabrocki^{6,7}, Shunhua Gui⁸, Guy Smaghe⁸, Troy D. Anderson⁴, Ronald J. Nachman⁶ & Yoonseong Park¹✉

The devastating *Varroa* mite (*Varroa destructor* Anderson and Trueman) is an obligatory ectoparasite of the honey bee, contributing to significant colony losses in North America and throughout the world. The limited number of conventional acaricides to reduce *Varroa* mites and prevent disease in honey bee colonies is challenged with wide-spread resistance and low target-site selectivity. Here, we propose a biorational approach using comparative genomics for the development of honey bee-safe and selective acaricides targeting the *Varroa* mite-specific neuropeptidergic system regulated by proctolin, which is lacking in the honey bee. Proctolin is a highly conserved pentapeptide RYLPT (Arg-Tyr-Leu-Pro-Thr) known to act through a G protein-coupled receptor to elicit myotropic activity in arthropod species. A total of 33 different peptidomimetic and peptide variants were tested on the *Varroa* mite proctolin receptor. Ligand docking model and mutagenesis studies revealed the importance of the core aromatic residue Tyr2 in the proctolin ligand. Peptidomimetics were observed to have significant oral toxicity leading to the paralysis and death of *Varroa* mites, while there were no negative effects observed for honey bees. We have demonstrated that a taxon-specific physiological target identified by advanced genomics information offers an opportunity to develop *Varroa* mite-selective acaricides, hence, expedited translational processes.

The *Varroa* mite (*Varroa destructor* Anderson and Trueman) is an obligatory ectoparasite of honey bees. Host expansion of the *Varroa* mite from the Eastern honey bee *Apis cerana* to the Western honey bee *A. mellifera* is associated with the worldwide dispersion of the mite in the last century¹ and has caused a major threat to the maintenance of healthy bee colonies². Infestation by *Varroa* mites causes direct damage to the bee colony and facilitates the transmission of pathogens^{3,4}. Control of the *Varroa* mite in beehives has relied heavily upon the use of synthetic and natural acaricides⁵.

The use of chemical acaricides in beehives to control *Varroa* mites requires stringent criteria. Finding selective acaricides that are nontoxic to honey bees is a challenging task because the arachnids and insects belong to the same phylum, Arthropoda, and diverged approximately 750 million years ago⁶. In addition, acaricides and their metabolized forms need to be without adverse effects on human health because of the consumption of the products in apiculture. Moreover, resistance to acaricides in the mites became another hurdle in the control of the *Varroa* mites^{7–10}. While new acaricidal compounds have been developed that show improved selectivity, new approaches have also been sought by taking advantage of the available genome sequences of the *Varroa* mite and honey bee and of new biotechnologies. For instance, RNA interference (RNAi) targeting the gene(s) specific to the *Varroa* mite has been tested for efficacy in apiculture¹¹. The RNAi strategy was combined with the engineered symbiont-mediated delivery of double stranded RNA¹². We have also proposed a new approach by targeting a *Varroa* mite-specific signaling system that is absent in honey bees¹³.

Our recent efforts included the development of highly selective acaricidal compounds using peptidomimetics targeting the neuropeptidergic system¹³. The rationale for this approach is based on comparative genomics between the *Varroa* mite and honey bee. A peptide signaling system that is present in *Varroa* mites but not in the

¹Department of Entomology, Kansas State University, 123 Waters Hall, Manhattan KS66506, USA. ²Department of Entomology, Punjab Agricultural University, Ludhiana 141004, India. ³Institute of Plant Protection, Shanxi Academy of Agricultural Sciences, 81 Longcheng Street, Taiyuan 030031, Shanxi, China. ⁴Department of Entomology, University of Nebraska, 103 Entomology Hall, Lincoln, NE 68583, USA. ⁵Department of Biochemistry and Molecular Biophysics, Kansas State University, Manhattan KS66506, USA. ⁶Insect Neuropeptide Laboratory, Southern Plains Agricultural Research Center, U.S. Department of Agriculture, 2881 F&B Road, College Station, TX 77845, USA. ⁷Institute of Organic Chemistry, Lodz University of Technology, 90-9024 Lodz, Poland. ⁸Lab Agrozoology, Department Plants and Crops, Ghent University, Coupure Links 653, 9000 Ghent, Belgium. ⁹These authors contributed equally: Vikas Jindal and Daqi Li. ✉email: ypark@ksu.edu

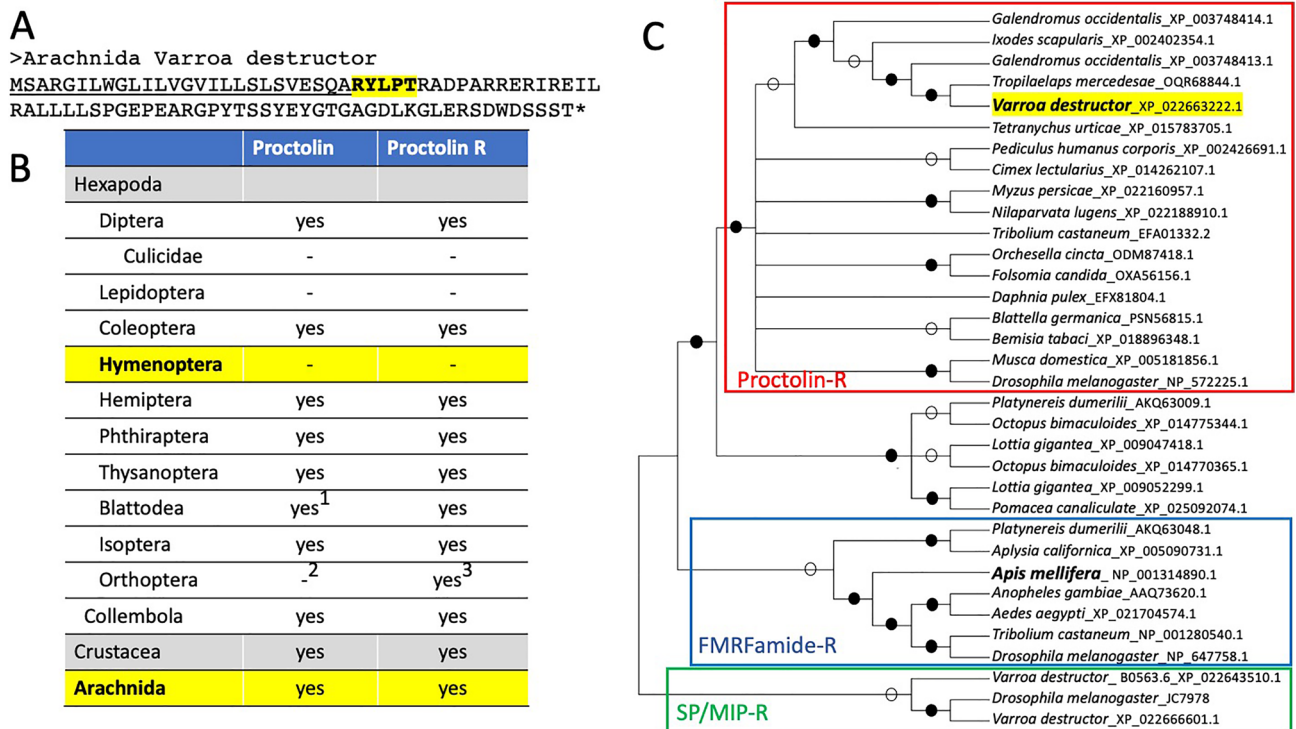


Figure 1. Taxonomic distribution of proctolin signaling system. The sequence of the proctolin of *Varroa destructor* (A), distribution of proctolin orthologous genes in arthropods (B) and phylogeny of the proctolin receptors rooted by FMRFamide receptors and sex peptide/myoinhibitory peptide receptors (C). The footnotes 1, 2, and 3, for Blattodea and Orthoptera proctolin is described in Supplementary data 1. Highlighted raw in B is for the taxonomic groups that is relevant to this study. Solid and empty circles in C are for bootstrapping values > 85% and > 50%, respectively.

honey bee genome could be an ideal target for this strategy. Previously, our study of peptidomimetics focused on two closely related neuropeptidergic systems¹³, namely, tachykinin-related peptide (TRP) and natalisin (NTL), where honey bees lack NTL and the NTL receptor. The study found that peptides carrying the C-terminal motif FWxxRamide are highly specific to interaction with the *Varroa* TRP receptor but not to the honey bee TRP receptor.

In this study, we applied a similar principle to the proctolin neuropeptidergic system, but without the complexity of two closely related peptidergic systems in NTL and TRP. Proctolin is a pentapeptide with the conserved sequence RYLPT (Arg-Tyr-Leu-Pro-Thr) and has been reported to elicit myotropic activity in many different arthropods. This peptide has thus far been found only in arthropods based on homologous sequences, and is absent in vertebrates. Interestingly, this peptide and the receptor have also not been found in Lepidoptera and Hymenoptera, including the honey bee, providing a highly selective acaricidal target. We tested a functionally expressed *Varroa* mite proctolin receptor against a series of proctolin analogs as well as peptidomimetics containing biostability enhancing components. In addition, we tested the proctolin mimetics, showing high activities on the receptor, for the oral toxicities on the *Varroa* mites. The current results show that proctolin peptidomimetics could represent a highly promising approach for the development of bee-safe acaricidal agents for the management of the *Varroa* mite.

Results and discussion

Arthropod proctolin and the G protein-coupled receptor. Proctolin and its receptors are widely distributed in arthropods, including insects, crustaceans, and arachnids (Fig. 1A–C, Supplementary Information). The *Varroa* mite gene encoding proctolin has a short open reading frame with a predicted N-terminal signal peptide. Immediately after the canonical signal peptide, the proctolin sequence followed and ended with a single R, a presumed monobasic cleavage site (Fig. 1A). In a survey of genes encoding proctolin in other taxa, almost all proctolin sequences identified in our search contained a strictly conserved pentapeptide followed by an R for monobasic cleavage with few exceptions.

The human louse (*Pediculus humanus*) contains the sequence RWLPT, where the second aromatic amino acid W2 replaced the aromatic Y2 in the consensus sequence. The rhinoceros beetle (*Oryctes borbonicus*) has RYLPA featuring a replacement of T5 with A5¹⁴. Lady beetles (*Coccinellidae*) encode for RYLST, replacing P4 with S4¹⁴. A previous study reported a RALPT variant (replacing Y2 with A2) in addition to the presence of the typical RYLPT in Colorado potato beetle (*Leptinotarsa decemlineata*)¹⁵. However, a search of the Colorado potato beetle genome¹⁶ identified only RYLPT, and the Y2 to A2 replacement was not identified in the Blast search algorithm (PAM30, E-value threshold: 100). Overall, natural variations of proctolin were found, but

with a limited number of cases involving the 4th or 5th amino acid residues, while W2 replacement retains the aromatic side chain in the tryptophan.

A proctolin receptor was first identified in *D. melanogaster*^{17,18} while the peptide proctolin was first described in the American cockroach in 1975¹⁹. In a phylogenetic analysis and in Blast searches for the proctolin receptor, an FMRFamide receptor was found to be the closest to the proctolin receptor group. The sex peptide receptor (also known as the myoinhibitory peptide or allatostatin B receptor) was the next closest group of G protein-coupled receptors (GPCRs, Fig. 1B). Interestingly, analysis of the basal lineages of Bilateria, lophotrochozoans including mollusks and annelids, revealed that a group of GPCRs were closely related to and grouped with the proctolin receptor of arthropods. Proctolin-like sequences in these taxa were not found in our blast searches. The authentic ligand for this group of receptors is expected to be similar to proctolin and remains to be uncovered.

In a survey of genome sequences, the *proctolin* gene was not identified in the insect orders Lepidoptera and Hymenoptera or the family Culicidae of the order Diptera, which includes mosquito species, important vectors of disease in human and animals. These species also lacked proctolin receptor orthologues. Based on the punctuated groups of taxa lacking proctolin and its receptor and the availability of many genome sequences for the species in these groups of insects, it is likely that they truly lack both proctolin and the receptors in independent evolutionary lineages. The translated sequences identified in the search are in Supplementary material 2.

In the case of Blattodea, where the first proctolin was isolated¹⁹ (Supporting information.1), the proctolin sequence was identified only in the genome sequence of *Zootermopsis nevadensis* (Blattodea; Isoptera). And, only a part of the prepropeptide encoding C-terminal amino acids lacking the N-terminal part of the mature proctolin sequence was identified in *Periplaneta americana*, *Blattella germanica*, and *Cryptotermes secundus* (Supplementary data). Proctolin receptors were also found in *Periplaneta americana*, (PGRX01000220.1: 583,757.0.612274) and in *C. secundus* (Blattodea; Isoptera, NEVH01012087.1: 3,622,722.0.3628892). The searches in the multiple species in Orthoptera genomes found similar results. The proctolin sequence was not identified in the genome sequences of Orthoptera, although proctolin was extensively studied in locust^{20–24}. Only a partial sequence covering the receptor ortholog was identified in *Laupala kohalensis* (NNCF01130566.1: 666,828.0.614799) and *Locusta migratoria* (AVCP010976312.1: 2376.0.2423). The identification of only partial sequences of *proctolin* genes and its receptor in Blattodea and Orthoptera is likely due to incomplete genome sequences and annotations, suggesting that these taxa likely retain the proctolin signaling pathway.

A number of previous reports contradicted what we found in the genome sequence survey, i.e., the lack of proctolin system in the Orders Lepidoptera and Hymenoptera. Proctolin immunoreactivity has been described in the gypsy moth²⁵ and *Manduca sexta*²⁶. A chromatographic isolation followed by cockroach hindgut bioassay described extremely low quantities of proctolin in honey bee and tent moth (*Malacosoma americana*): 0.12 and 0.17 mg/kg of tissue, respectively²⁷. Proctolin activity on the *Bombyx mori* larval gut has been previously found, though an extremely high concentration of 180 μ M is required for hindgut contraction, and 10 μ M is required in the midgut to slightly reduce leucine uptake²⁸. In the honey bee, an extremely high dose of proctolin delivered via injection, 1 μ L containing 1 μ g (1.54 nmoles), increased the egg-laying activity of the queen²⁹. However, in these studies, the bioactivity was very weak with extremely high concentrations of proctolin required for the bioactivities. The bioactivities described in these studies are unlikely a consequence of the natural endogenous bioactivities of proctolin.

Proctolin-receptor docking model. To study the activities of proctolin peptidomimetics, we investigated the receptor by in silico docking modes and in vitro assays on the heterologously expressed *Varroa* mite proctolin receptor in Chinese Hamster Ovarian (CHO) cell that has been established for various insect GPCR expression^{30,31}. The structure of proctolin receptor was built using the GPCR I-TASSER (Iterative Threading ASSEmby Refinement) server^{32–35}, and the docking with proctolin was simulated by an Induced Fit Docking (IFD) method³⁶. A QM-Polarized Ligand Docking method revealed the binding pocket of the proctolin receptor (Fig. 2). The docking model shows the N-terminal Arg1 and Tyr2 of the ligand interacted with the Tyr99 and Arg111, respectively, by forming cation- π interactions with the distances 3.9 and 3.6 Å (Fig. 2A). These first two residues of proctolin are found to be important for access to the binding site and anchoring to dock into the receptor pocket. Cation- π interactions, a strong noncovalent binding interaction, appear to play unique and important role for proctolin docking on the ligand binding pocket. We also found that the extracellular surface of the receptor and the binding pocket including the region accommodating the positively charged Arg1 of the proctolin are generally negatively charged (Fig. 2B).

The importance of cation- π interactions was further supported in the mutagenesis of the proctolin ligand and proctolin receptor. The changes in Tyr2 of proctolin to other natural and non-natural aromatic amino acids generally retained the activities on the receptor in general (Table 1 and Fig. 2C), whereas Tyr2 to Ala mutation almost abolished the activity of the ligand (Table 1). Interestingly, however, the R111A (Arg111 to Ala) and R111K mutations on the receptor, which is the predicted receptor residue interacting with Tyr2 of the ligand, caused only minor changes in the receptor activities to the proctolin mimetics. These results imply that the aromatic ring in the Tyr2 interacts not only with the binding pocket, but functions for accessibility to the binding site. The cation- π interactions predicted for Arg1 of proctolin with Y99 of the receptor is supported by the mutations of the receptor Y99A and Y99F. The Y99F-mutated receptor with the aromatic residue maintained the activities, whereas Y99A lost the activities to various proctolin and its mimetics. The roles of cation- π interactions in the ligand binding sites and the amino acid residues lining the active site gorge need to be further studied.

Activities of proctolin analogs on the *Varroa* mite proctolin receptor. The receptor expressed in the heterologous expression system showed strong reactivity to proctolin, exhibiting an EC₅₀ of 0.24 nM

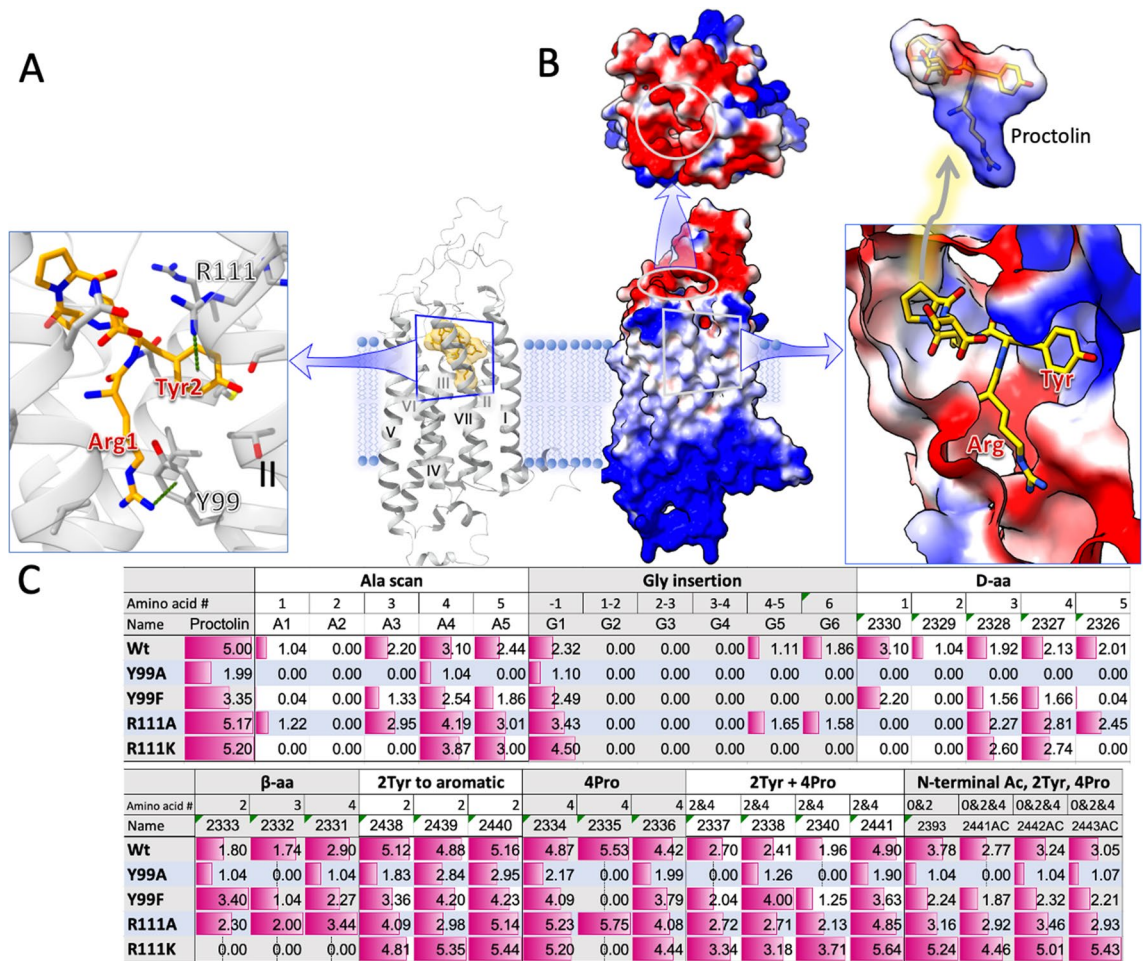


Figure 2. In silico docking model. The importance of cation- π interactions of Arg1 and Tyr2 of the proctolin (A), the charges of receptor and ligands on the docking model (B), and the mutated ligands and receptor activities tested on the receptors expressed in the CHO cell (C). In B, blue is for positive and the red is for negative charges. In C, the values are normalized values for the log₁₀-based scale activities relative to the 5 as the standard for wild-type receptor with the proctolin.

(Table 1). The negative control, transfection of the empty vector, did not show any activity at a high concentration of 10 μ M proctolin. The receptor was also tested with a variety of peptide analogs and peptidomimetics.

An alanine scan series of analogs was evaluated to determine the importance of the side chains of specific amino acid residues (Table 1). The first two amino acids R1 and Y2 are the most important, while the fourth residue P4 can be replaced by A with only minor loss of the activity of the receptor. The replacement of the third and fifth amino acids (L3 and T5, respectively) to A resulted in moderately reduced activity. Therefore, the first two amino acids R and Y likely contain side chains that interact strongly with the receptor. We used glycine insertions to examine the importance of any two consecutive amino acid residues. The insertion of G at the position between R1 and Y2 and between Y2 and L3 dramatically reduced the activity (Table 1 and Fig. 3). All other G insertions resulted in significant reductions in activity except the N-terminus attachment of G, which resulted in a minor loss in activity (Table 1 and Fig. 3). The space in the N-terminus may allow chemical modification that offers increased permeability and blocks the aminopeptidase N mediated degradation³⁷ of the proctolin peptidomimetics.

Activities of proctolin peptidomimetics on the Varroa mite proctolin receptor. A series of peptidomimetic analogs of proctolin were chosen for synthesis and receptor evaluation that incorporated components that can enhance resistance to peptidase enzyme hydrolysis, i.e., biostability (including such enzymes as ACE, neprilysin, and aminopeptidases). The first set of five analogs involved sequential replacement of each of the amino acid residues with a D-amino acid. D-amino acids are not recognized by peptidase enzymes and can confer peptidase resistance to adjacent peptide bonds. Most D-amino acid replacements led to significant loss of potency, with the major exception being the replacement of the N-terminal R with dR in 2330, which retained activity at 8.6 nM for the EC₅₀ (Table 1). This modification is of importance as it can protect the N-terminus from aminopeptidase degradation.

A. First set of peptidomimetics

| Chemical ID | Sequence | EC ₅₀ | 95% CI | Fold change |
|------------------------|------------------|------------------|-----------------|-------------|
| Proctolin | RYLPT | 0.2439 | 0.1362 - 0.4546 | 1 |
| Alanine scan | | | | |
| A1 | AYLPT | 956.5 | 779.0 - 1172 | 3921.7 |
| A2 | R ALPT | 1640 | 1223 - 2233 | 6724.1 |
| A3 | RY APT | 92.68 | 31.25 - 258.5 | 380.0 |
| A4 | RYL AT | 5.402 | 1.157 - 21.98 | 22.1 |
| A5 | RYL PA | 42.02 | 13.88 - 115.3 | 172.3 |
| Glycine insert | | | | |
| G1 | G RYLPT | 48.71 | 17.73 - 120.2 | 199.7 |
| G2 | R G YLPT | 17475 | 8538 - 308933 | 71648.2 |
| G3 | RY G LPT | 22319 | 3934 - ? | 91508.8 |
| G4 | RYL G PT | 1328 | 1194 - 1478 | 5444.9 |
| G5 | RYLP G T | 755 | 439.7 - 1241 | 3095.5 |
| G6 | RYLPT G | 997.1 | 713.3 - 1382 | 4088.2 |
| Peptidomimetics | | | | |
| 2326 | RYLP[dT] | 1867 | 1451 - 2443 | 7654.8 |
| 2327 | RYL[dP]T | 458.8 | 199.9 - 973.1 | 1881.1 |
| 2328 | RY[dL]PT | 136.3 | 108.2 - 172.3 | 558.8 |
| 2329 | R[dY]LPT | 201.1 | 116.9 - 363.1 | 824.5 |
| 2330 | [dR]YLPT | 8.584 | 4.435 - 16.55 | 35.2 |
| 2331 | RYL[β3P]T | 7.878 | 3.729 - 16.12 | 32.3 |
| 2332 | RY[β3L]PT | 161.4 | 104.8 - 254.8 | 661.7 |
| 2333 | R[β3F]LPT | 139.5 | 60.76 - 348.0 | 572.0 |
| 2334 | RYL[HyP]T | 0.6811 | 0.1287 - 3.408 | 2.8 |
| 2335 | RYL[Aib]T | 2.675 | 0.4071 - 22.78 | 11.0 |
| 2336 | RYL[Oic]T | 1.832 | 0.3699 - 13.52 | 7.5 |
| 2337 | R[dY]L[HyP]T | 34.99 | 14.52 - 82.02 | 143.5 |
| 2338 | R[β3F]L[HyP]T | 33.2 | 14.19 - 76.76 | 136.1 |
| 2340 | R[dY]L[Oic]T | 129.2 | 84.59 - 200.1 | 529.7 |

B. Second set of peptidomimetics

| | | | | |
|----------------|---|-------|----------------|------|
| Proctolin | RYLPT | 23.97 | 2.059 - 345.8 | 1.0 |
| 2438 | R[Phe(4-F)]LPT | 16.67 | 2.766 - 146.3 | 0.7 |
| 2439 | R[Phe(4-NO ₂)]LPT | 10.27 | 0.1075 - 215.1 | 0.4 |
| 2440 | R[Phe(4-Cl)]LPT | 5.728 | 3.750 - 8.657 | 0.2 |
| 2441 | R[Phe(4-F)]L[HyP]T | 16.96 | 7.301 - 42.36 | 0.7 |
| Ac-2441 | Ac-R[Phe(4-F)]L[HyP]T | 1473 | 1034 - 2128 | 61.5 |
| Ac-2442 | Ac-R[Phe(4-NO₂)]L[HyP]T | 500.9 | 99.89 - 1902 | 20.9 |
| Ac-2443 | Ac-R[Phe(4-Cl)]L[HyP]T | 898.1 | 6.843 - ? | 37.5 |

Table 1. Activities of proctolin and its mimetics on the *Varroa* mite proctolin receptor. The modified amino acids are in red in the amino acid sequences. Bold and underlined peptidomimetics are the ones further studied in feeding assay. [d] is for D- amino acid, [β3] is for beta -3 amino acids, [Hyp] is for hydroxy proline, [Aib] is for 2-amino butyric acid, and [Oic] is for octahydroindole-2-carboxylic acid, and [Phe-4] is for modified phenylalanine at the 4 position. Note that the second set of peptidomimetics were tested on the cells selected for stable expressions of the receptor showing significantly lower activity to proctolin and to other analogues than those in the first set using the cells with transient expression of the receptor.

A set of analogs involved the replacement of amino acid residues with β-amino acids (Table 1); which are also not recognized by peptidases and can confer resistance to adjacent peptide bonds to enzyme hydrolysis. The amino acids chosen for replacement depended on the commercial availability of appropriate β-amino acids. Thus, L and P were replaced with β³L (2332) and β³P (2331), respectively. Finally, the aromatic Y residue was replaced with aromatic β³F (2333). Of these three analogs, analog 2331 (β³P for P) retained high potency with an EC₅₀ of 7.9 nM.

The P (Pro) amino acid is an important residue for the stabilization of secondary structures such as β-turns, and this property was therefore retained in each of the members of the next series of analogs. Here, the P was replaced with either a modified, sterically-hindered proline analogs hydroxyproline (Hyp) and octahydroindole-2-carboxylic acid (Oic), or the sterically-hindered, turn-promoting residue aminoisobutyric acid (Aib). One analog in this set also incorporates an acetyl group (Ac) at the N-terminus to increase resistance to aminopeptidase attack. As observed with the high activity retained by analog 2331 (β³P for P), these P4 replacement analogs similarly demonstrated high potency retention. Analog 2334 (with Hyp) exhibited high potency with an EC₅₀ of 0.68 nM, only 2.8 times less potent than the natural peptide. This analog also previously showed high activity in in vivo proctolin myotropic assays^{38–45}. Analogs 2336 (with Oic) and 2335 (with Aib) also retained relatively

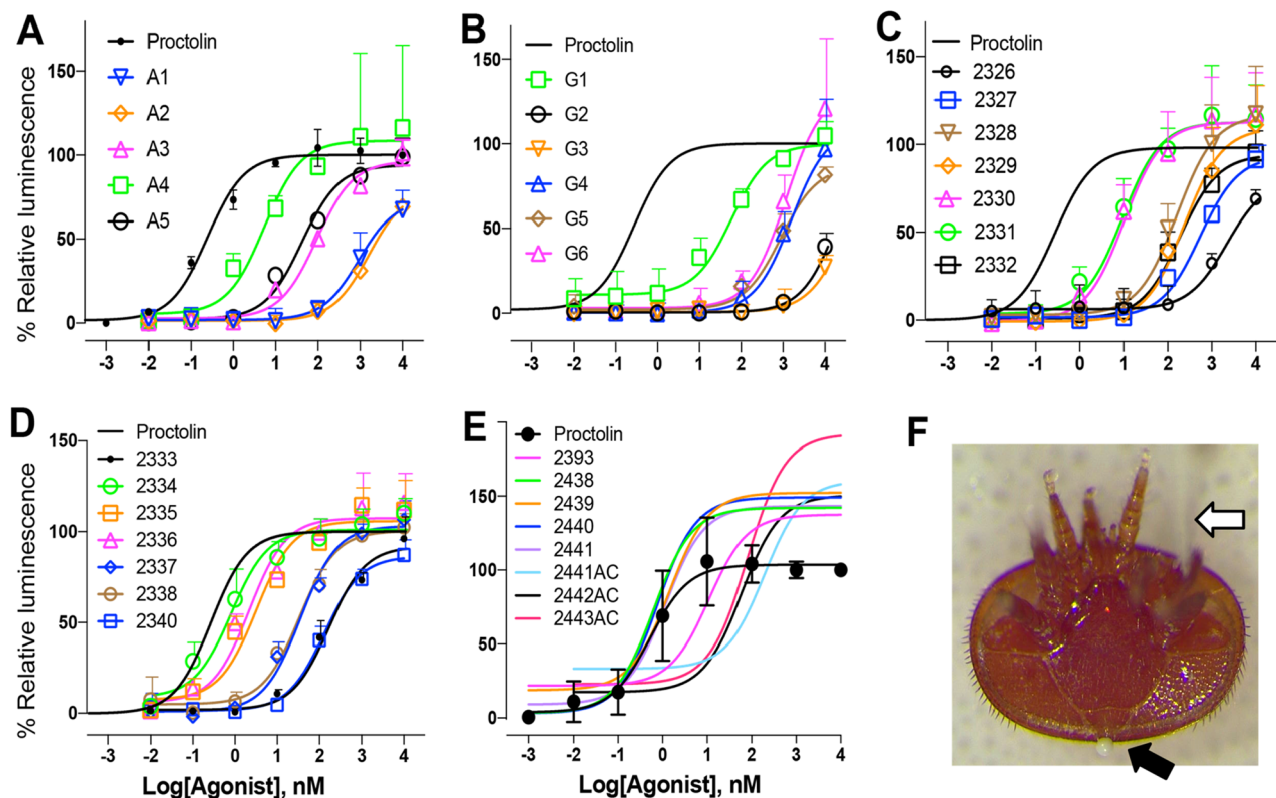


Figure 3. Activities of proctolin peptidomimetics. Log-dose response curves showing the activities of proctolin analogs and peptidomimetics on the *Varroa destructor* proctolin receptor (A to E), and *Varroa* mite showing excretion induced by injection of proctolin solution (F). In F, the white arrow is for the location of microinjection needle and the black arrow shows the excretion from the anus of *Varroa* mite.

strong potencies in the nanomolar range, with EC_{50} 's of 1.8 and 2.7 nM, respectively. These sterically-hindered Pro replacements can confer greater biostability to the analogs that incorporate them^{46,47}.

Additional analogs featured double-replacement analogs to potentially confer enhanced peptidase resistance to every peptide bond in the proctolin sequence. A component that enhances stability is adjacent to each peptide bond in the sequence of this analog pair. In this pair, sterically-hindered P replacements were coupled with either a replacement of Y with dY (2337 or 2340) or with β^3F (2338). Despite the major modifications incorporated into analogs 2338 (R[β^3F]L[HyP]T) and 2337 (R[dY]L[HyP]T), the two retained full efficacy (maximal response) and a relatively strong potency with EC_{50} 's of 33 and 35 nM, respectively. Indeed, in each case, the potency of these double-replacement analogs at positions Y2 and P4 exceeded that of the corresponding analog (2333 and 2329, respectively) with only a single replacement at the Y2 position by a factor of 8 and 4, respectively. Analog 2340 (R[dY]L[Oic]T) was less potent than 2337 and 2338 by approximately an order of magnitude. Mimetic analogs featuring enhanced biostability have an advantage over native peptides in that they can exist and remain active for a longer period in the hemolymph. The analogs 2338 and 2337 may provide leads for biostable mimetic analogs that can disrupt the processes mediated by proctolin in parasitic mites.

The last set (the second set in Table 1) of peptidomimetic tested were the proctolin variants at the Y2 position with phenylalanine carrying the aromatic ring with 4-F, 4-NO₂, 4-Cl, and with additional variations for [HyP] replacing at the 4th P and for Ac at the N-termini. This set of peptidomimetics showed high activities including hyper activities that have higher activities than endogenous proctolin, although the second set of ligands tested on the cells selected for stable expressions of the receptor showed significantly lower activity with two orders of magnitude to proctolin and to other analogues (Table 1 and Fig. 3). Replacement of the Y2 to [Phe(4-NO₂)], [Phe(4-Cl)], [Phe(4-F)], [Phe(4-F)] showed even higher activities than proctolin. A double-replacement, R[Phe(4-F)]L[HyP]T, also had higher activity than proctolin, while it had slightly reduced activity than the single replacement R[Phe(4-F)]LPT (Table 1).

An interesting observation in this study is that the highly active ligands often display higher efficacy (maximal response) than proctolin at high concentrations (Fig. 3). A4, G6, 2330, 2331, 2334, and 2336 are in this category; the activities of these ligands at the 1 μ M and 10 μ M were higher than that of proctolin. Previous studies proposed that binding of the agonist and elicitation of conformational changes to initiate activation of downstream responses are sequentially distinctive processes in the β_2 adrenoceptor^{48–50}. The highly active ligands in this study may also have influenced receptor activation of the proctolin receptor in a similar fashion. Certain configurations of the ligand may elicit more efficient conformational changes in the receptor than the endogenous ligand, despite featuring lower binding kinetics.

The activities of numerous proctolin peptidomimetics have been previously tested in various biological systems^{38–45}. The major systems used for assessing the bioactivities of peptidomimetics were assays for cardioacceleration, gut motility, and oviduct motility in cockroach, locust, and beetle species. The results of these studies allow an excellent comparison to the results of our study using the proctolin receptor to directly assess the activities of the peptidomimetics. We find a general consensus in comparisons between our peptidomimetics in *Varroa* mite receptor activity and earlier studies using assays on myotropic activities in other species of insects. In Table 1, the peptidomimetics with gray backgrounds were inactive, and the bold and underlined ones were active in the earlier bioassay systems. Generally, where comparisons can be made, the peptidomimetics with a < 50 nM EC₅₀ were also active in one of the early bioassay systems, with the exception of the R1 replacement by dR, which had an EC₅₀ of 5.62 nM, only 26 × lower than native peptide activity, but no activity in earlier in vivo bioassays. This exception and difference could be due to structural variations between the receptors in the different species.

A previous study has demonstrated that the replacement of Y2 with analogs of Y or F incorporating modifications at the aromatic ring led to highly active proctolin analogs, in some cases with even higher activities than that of endogenous proctolin in the bioassay systems. This suggests that future studies investigating similar modifications of the aromatic moiety at the Y2 position could lead to biostable mimetic proctolin analogs with even greater potency and efficacy on the *Varroa* mite receptor.

Peptidomimetics toxicity to *Varroa* mites and to the honey bee. Four peptidomimetics tested for the bioassays were three strong agonists 2334, 2336, and Ac-2442, and an inactive agonist 2326 determined on the *Varroa* mite proctolin receptor. Initially, the highly active agonist 2334 on the receptor was directly injected into the body cavity (~ 5 nL of 200 μM) to test the direct biological activities. The injection immediately induced excretion of a drop of fecal material through the anus (3/4 individuals) while the H₂O control did not cause excretion or other noticeable change (0/4, Chi-square test $p < 0.05$). This result indicates that the *Varroa* mite proctolin activity includes activation of excretory system which is a well-documented activity in other insects although the study needs to be further expanded. In the continued bioassay, the toxicities were assessed by counting paralysis/death in feeding assay. A drop of 200 nL solution was placed on the gnathosoma of an immobilized mite for forced feedings of active components. Low levels of acute toxicities of peptidomimetics were indicated by lower than 50% effects within 6 h after the treatments. The toxic effects were increased over time and reached 100% of the effects in the 48 h treatments of 2336 (Fig. 4, ANOVA $p < 0.05$). In H₂O control, about 10% or less of the number of individuals were paralyzed/dead. Accurate cause of the paralysis/death remains yet to be studied.

Acute toxicity of the peptidomimetics on the worker honey bee was tested for 2439, 2334, 2336, Ac-2442, and H₂O control by injections of the compounds into thorax. Injections of 50 nL solutions at the 200 μM concentrations did not show any negative effects in 24 h observations after the injections ($n = 4$ for each compound). The assay was expanded to study potentially a longer effect on the honey bee by 7 days of treatments for compounds 2330, 2331, 2334, 2335, and 2336. We found no statistically significant differences in sugar consumption rate and survival (Table 2).

In addition, the activities of the proctolin peptidomimetics were tested on the honey bee FMRFamide receptor that is the most closely related to the proctolin receptor (Fig. 1). Honey bee FMRFamide receptor was cloned and expressed in the same system as described for the proctolin receptor. Proctolin and its peptidomimetics show no activities while the honey bee FMRFamides showed strong activities on the honey bee FMRFamide receptor.

Conclusions

A new approach to developing selective acaricidal compounds targeting a *Varroa* mite specific neuropeptidergic system is outlined in this study. We have successfully developed an assay system using the *Varroa* mite proctolin receptor. Peptidomimetics were shown to retain relatively strong activity on the *Varroa* mite receptor and provide guidelines for the development of 2nd generation analogs of higher activity and bioavailability. In particular, two analogs that feature double replacements offer enhanced peptidase protection to all peptide bonds and retain full efficacy and significant retention of potency and represent promising lead analogs. The peptidomimetics pre-selected by the receptor assays showed significant activities in *Varroa* mite feeding assays at very low concentrations while high concentrations of the peptidomimetics in honey bee found no detectable adverse effects.

Methods

Chemicals. Proctolin and the amino acid replacement, alanine scan and glycine insertion analogs were synthesized by Pepmic (Jiangsu, China) and prepared for greater than 85% purity. For Chinese hamster ovarian (CHO) cell culture, DMEM/F12 medium, Fungizone® and penicillin/streptomycin were obtained from Gibco® Cell Culture at Life Technologies (Grand Island, NY). Coelenterazine h was obtained from ATB Bioquest (Sunnyvale, CA). Fetal bovine serum (FBS) was obtained from Atlas biologicals (Fort Collins, CO).

Bioinformatics and receptor cloning. Proctolin and the receptor searches in GenBank were made by an initial query of the respective protein sequence of *Drosophila melanogaster*. When the search yielded orthology in various taxa, further expanded searches were made by using queries of closely related taxa. In the case of the proctolin receptor orthology searches, two criteria were used: back blast of the search output against the *D. melanogaster* database and clustering in the distance tree view. “Lacking” orthology was concluded after searches of the NCBI database for nr proteins, the RefSeq Genome Database, whole-genome shotgun contigs, and expressed sequence tags during December 2018.

The receptor cDNA was amplified from the total RNA isolated from a pool of 10 adult mites collected from beehives in Manhattan, Kansas¹⁵. Total RNA was isolated by using TRI Reagent (Zymo Research). First-strand

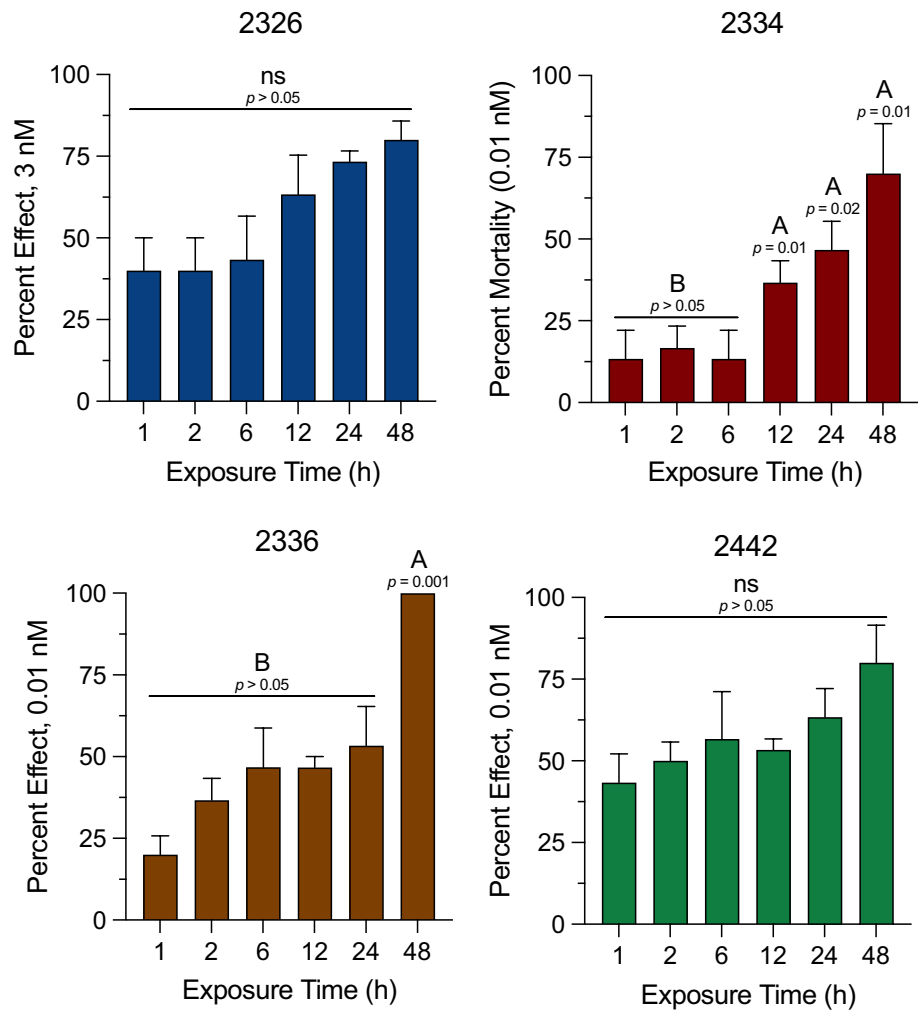


Figure 4. Proctolin peptidomimetics activities. Time-dependent efficacy of peptide mimics to *Varroa* mites. Immobilized Female *Varroa* mites were topically treated on the gnathosoma; 2326 at 3 nM and 2334, 2336, and 2442 at 0.01 nM and the number of mites affected (i.e., paralyzed or dead) was recorded for 1 to 48 h post-treatment. Vertical bars represent the mean \pm standard error. Different letters above the bars indicate a significant difference between the mean percent effect at each time point using a one-way ANOVA with a Tukey’s post-hoc test ($p < 0.05$). The mortalities in water controls were $\sim < 10\%$ at 48 h exposure.

| Analogue | n | Survival (%) | Amount of sugar water uptaken per bee in 3 days (mean \pm SD, mg) |
|---------------|----|--------------|---|
| Water control | 30 | 70 | 279 \pm 65 |
| Proctolin | 30 | 73 | 278 \pm 58 |
| No-injection | 30 | 77 | 272 \pm 51 |
| 2334 | 30 | 73 | 281 \pm 52 |
| 2331 | 30 | 70 | 271 \pm 67 |
| 2336 | 30 | 70 | 283 \pm 55 |
| 2335 | 30 | 60 | 273 \pm 46 |
| 2330 | 30 | 63 | 289 \pm 69 |

Table 2. Percent survival of honey bee (*Apis mellifera*) and amount of sugar water uptake after injections of proctolin analogs. Sugar water consumption was measured at the day 3 and the survival was counted in the seventh day after treatment. The statistics were a Chi-square test for the survivorship and Student’s t-test for the sugar water consumption. No statistical difference compared to the water control was found at the $P = 0.05$.

cDNA was synthesized by using an ImProm-II™ Reverse Transcription System (Promega), and PCR amplification was performed by Q5® high-fidelity DNA polymerase (New England Biolabs). The PCR product was cloned into pGEM-T-EZ (Promega) and transferred to pcDNA3.1+ (Invitrogen) to add the *EcoRI* cloning site. The sequence was confirmed by Sanger sequencing and submitted to GenBank (Accession number MN462557.1). Phylogenetic tree was generated by using neighbor joining method with 1000 bootstrapping after alignment made by Muscle in MEGA7⁵¹.

Receptor activity assay. Cells were transiently transfected with pcDNA3.1+ containing the open reading frame of *Varroa* mite proctolin receptor (VdProctR) or empty vector using TransIT®-2020 (Mirus Bio). Approximately thirty hours after transfection, the cells were collected and preincubated with coelenterazine h for the functional assay, as previously described^{30,31,52}. The ligands in serial dilutions were loaded into 96-well opaque plates. Cells treated with coelenterazine h were injected into each well on an Orion microplate luminometer (Berthold) luminescent plate reader. The luminescence was measured for 20 s immediately after the cell injections. Data analyses were performed to determine the accumulated luminescence value for 20 s after extraction of blank-well luminescence. A dose–response curve was generated and the EC₅₀ (50% effective concentration) was calculated in Origin 7 (OriginLab) as described in Jiang et al.^{31,53}. The three biological replications were regressed for the dose–response curves with 95% confidence intervals (Table 1). For the tests of the second set of ligands, we used the cell line that stably expressed VdProctR, which were selected by Zeocin for 5 passages.

Toxicity test. Adult female *Varroa* mites were collected using a sugar roll method from honey bee hives located at the East Campus apiary of the University of Nebraska (Lincoln, NE USA) in September–October 2019. The hives were not treated with chemicals for honey bee parasites or pathogens. The mites were sorted in the laboratory with a paint brush and tested within 4 h post collection. Only healthy mites, vigorously mobile on the filter paper, were placed in 9 cm diameter Petri dishes (Fisher Scientific) lined with filter paper. The dorsal side of the mites was secured to a strip of tape placed on the filter paper. Ten mites were secured to the tape in each dish and three dishes were used for each treatment (i.e., 30 mites/treatment). The peptide mimics were prepared for 25 mM stock solution in dimethyl sulfoxide (DMSO) and further dilutions were made in autoclaved ddH₂O to a concentration of 0.1 nM for 2334, 2336, and Ac-2442 and 3 nM for 2326. Each peptide mimic was delivered as a 200 nL aliquot to the gnathosoma of the mites with autoclaved ddH₂O serving as the untreated control. Following exposure to the peptide mimics, the mites were kept at high humidity for 48 h. The number of affected (i.e., dead and/paralyzed) was observed and recorded at 1, 2, 6, 12, 24, and 48 h. The percent effect for each treatment was analyzed using a one-way analysis of variance (ANOVA) with a Tukey's post-hoc test (GraphPad Prism, La Jolla, CA; $p < 0.05$).

For injection experiments in *Varroa* mite to examine the direct physiological response to the peptidomimetics, we injected ~5 nL of 200 μM compound 2334 while controls were injections of equal volume of H₂O ($n = 4$ in each). Micro-glass electrodes were used for the injections using the pressure injection system (Dagan PMI-200) through anterior region of ventral idiosoma (Fig. 3F). The injections were made within 5 h after the collections of the mites as described above. Defecation induced by the injection was observed within 10 min.

For honey bee (*Apis mellifera*) assays, honey bee workers from healthy colonies were collected from Honeybee Valley of Ghent University, Belgium, and maintained in cages on sugar dough and water, under standardized conditions of 28–30 °C, 60–65% air humidity and continuous darkness⁵⁴. The colony were maintained with a periodic sanitary control that the honeybee hives are free of pathogens, diseases and viruses. There was no *Varroa* mite infection in the honeybee hives at the moment of collecting the workers for the assays. In the preliminary/first assay, honeybee workers were injected with 10 pmol of proctolin or the proctolin analogue. This was realized by injecting a volume of 50 nL of a concentration of the compound of 200 μM. Potential effects on survival were scored at 24 h after injection. There were no lethal effects. This test was done with the following compounds were tested: 2439, 2334, 2336, Ac-2442 and controls. Subsequently, working solutions were freshly prepared prior to the bioassays by diluting the stock with distilled water to the required concentration.

In the second assay the honeybee workers were injected with 12 pmol of proctolin or the proctolin analogues. This was realized by injecting a volume of 800 nL of a concentration of the compound of 15 μM. Potential effects were scored: sublethal effects on food intake at 3 days after injection (sugar water uptake) and also survival at day 7 after injection (Table 2). This test was done the following compounds: 2330, 2331, 2334, 2335, 2336, proctolin, and controls. The controls were injected with the same amount of distilled water and a non-injected control was included as described before⁵⁵. In brief, after injecting, each honey bee was reared individually with 50% sugar water (BioGluc, Biobest, Westerlo, Belgium) in a single housing tube, and the food intake of each honeybee was measured at 72 h after treatment (Table 2). The reduction of sugar water represented the amount of food intake by the honey bee within 3 days. Per treatment, two independent repetitions were performed, each consisting of 15 honey bees.

Peptidomimetic analog synthesis. Analogs were synthesized on an ABI 433A peptide synthesizer with a modified FastMoc 0.25 procedure using an Fmoc-strategy starting from Rink amide resin (Novabiochem, San Diego, CA, 0.5 mM/g). The Fmoc protecting group was removed by 20% 4-methyl piperidine in DMF (Dimethyl formamide). A fourfold excess of the respective Fmoc-amino acids was activated in situ using HBTU (2-(1-h-benzotriazol-1-yl)-1,1,3,3-tetramethyluronium hexafluorophosphate) (1 eq.) /HOBt (1-hydroxybenzotriazole) (1 eq.) in NMP (N-methylpyrrolidone) or HATU (2-(7-Aza-1H-Benzotriazole-1-yl)-1,1,3,3-tetramethyluronium hexafluorophosphate) (1 eq.) /HOAt (1-hydroxy-7-azabenzotriazole) (1 eq.) in NMP for Aib and the amino acid immediately following it in the sequence. The coupling reactions were base catalyzed with DIPEA

(N,N-diisopropylethylamine) (4 eq.) The amino acid side chain protecting groups were PMC for Arginine and tBu for both Threonine and Tyrosine. Acetylation was accomplished as previously described⁵⁶.

The analogs were cleaved from the resin with side-chain deprotection by treatment with TFA (Trifluoroacetic acid):H₂O:TIS (Triisopropylsilane) (95.5:2.5:2.5 v/v/v) for 1.5 h. The solvents were evaporated by vacuum centrifugation and the analogs were desalted on a Waters C₁₈ Sep Pak cartridge (Milford, MA) in preparation for purification by HPLC. The analogs were purified on a Waters Delta-Pak C₁₈ reverse-phase column (8 × 100 mm, 15 μm particle size, 100 Å pore size) with a Waters 510 HPLC system with detection at 214 nm at ambient temperature. Solvent A = 0.1% aqueous trifluoroacetic acid (TFA); Solvent B = 80% aqueous acetonitrile containing 0.1% TFA. Initial conditions were 10% B followed by a linear increase to 90% B over 40 min.; flow rate, 2 ml/min. Delta-Pak C₁₈ retention times: **2393**, Ac-RYL[**Hyp**]T-OH: 3.0 min; **2336**, RYL[**Oic**]T-OH: 3.0 min; **2330**, [dR]YLPT-OH: 2.4 min; **2331**, RYL[β³P]T-OH: 2.8 min; **2335**, RYL[**Aib**]T-OH: 2.4 min; **2337**, R[**dY**]L[**Hyp**]T-OH: 2.5 min; **2327**, RYL[**dP**]T-OH: 2.6 min; **2328**, RY[**dL**]PT-OH: 2.6 min; **2326**, RYLP[**dT**]T-OH: 2.1 min; **2329**, R[**dY**]LPT-OH: 2.4 min; **2332**, RY[β³L]PT-OH: 2.5 min; **2333**, R[β³F]LPT-OH: 2.5 min; **2334**, RYL[**Hyp**]T-OH: 2.4 min; **2340**, R[**dY**]L[**Oic**]T-OH: 2.4 min. The analogs were further purified on a Waters Protein Pak I 125 column (7.8 × 300 mm). Conditions: isocratic using 80% acetonitrile containing 0.1% TFA; flow rate, 2 ml/min. Waters Protein Pak retention times: **2393**, Ac-RYL[**Hyp**]T-OH: 7.0 min; **2336**, RYL[**Oic**]T-OH: 7.0 min; **2330**, [dR]YLPT-OH: 7.0 min; **2331**, RYL[β³P]T-OH: 7.0 min; **2335**, RYL[**Aib**]T-OH: 7.0 min; **2337**, R[**dY**]L[**Hyp**]T-OH: 7.5 min; **2327**, RYL[**dP**]T-OH: 7.0 min; **2328**, RY[**dL**]PT-OH: 7.5 min; **2326**, RYLP[**dT**]T-OH: 7.5 min; **2329**, R[**dY**]LPT-OH: 7.0 min; **2332**, RY[β³L]PT-OH: 6.5 min; **2333**, R[β³F]LPT-OH: 6.5 min; **2334**, RYL[**Hyp**]T-OH: 7.5 min; **2340**, R[**dY**]L[**Oic**]T-OH: 7.5 min.

Amino acid analysis was carried out to quantify the analogs and to confirm identity: **2393**, Ac-RYL[**Hyp**]T-OH: L[1.0], R[1.0], T[1.0], Y[1.0]; **2336**, RYL[**Oic**]T-OH: L[1.0], R[1.0], T[1.0], Y[1.1]; **2330**, [dR]YLPT-OH: L[1.0], P[1.2], R[1.0], T[1.0], Y[1.1]; **2331**, RYL[β³P]T-OH: L[1.0], R[1.0], T[1.0], Y[1.1]; **2335**, RYL[**Aib**]T-OH: L[1.0], R[0.9], T[1.0], Y[1.1]; **2337**, R[**dY**]L[**Hyp**]T-OH: L[1.0], R[0.9], T[1.0], Y[1.1]; **2327**, RYL[**dP**]T-OH: L[1.0], P[1.0], R[1.0], T[1.0], Y[1.0]; **2328**, RY[**dL**]PT-OH: L[1.0], P[1.0], R[1.0], T[1.0], Y[1.0]; **2326**, RYLP[**dT**]T-OH: L[1.0], P[1.0], R[1.0], T[1.0], Y[1.1]; **2329**, R[**dY**]LPT-OH: L[1.0], P[1.0], R[1.0], T[1.0], Y[1.1]; **2332**, RY[β³L]PT-OH: P[1.1], R[1.0], T[1.0], Y[1.0]; **2333**, R[β³F]LPT-OH: L[1.0], P[0.9], R[0.9], T[1.0]; **2334**, RYL[**Hyp**]T-OH: L[1.0], R[1.0], T[1.1], Y[1.0]; **2340**, R[**dY**]L[**Oic**]T-OH: L[1.0], R[1.0], T[1.1], Y[1.0]. The identity of the analogs was also confirmed by MALDI-MS on a Kratos Kompact Probe MALDI-MS instrument (Shimadzu, Columbia, Maryland). The following molecular ions (MH⁺) were observed: **2393**, Ac-RYL[**Hyp**]T-OH: 708.1 (calc. 708.0); **2336**, RYL[**Oic**]T-OH: 704.8 (calc. 703.9); **2330**, [dR]YLPT-OH: 649.8 (calc. 649.7); **2331**, RYL[β³P]T-OH: 663.6 (calc. 663.0); **2335**, RYL[**Aib**]T-OH: 637.6 (calc. 637.7); **2337**, R[**dY**]L[**Hyp**]T-OH: 665.6 (calc. 655.8); **2327**, RYL[**dP**]T-OH: 649.7 (calc. 649.7); **2328**, RY[**dL**]PT-OH: 649.7 (calc. 649.7); **2326**, RYLP[**dT**]T-OH: 649.3 (calc. 649.0); **2329**, R[**dY**]LPT-OH: 649.7 (calc. 649.7); **2332**, RY[β³L]PT-OH: 663.5 (calc. 663.0); **2333**, R[β³F]LPT-OH: 647.4 (calc. 647.0); **2334**, RYL[**Hyp**]T-OH: 665.8 (calc. 665.7); **2340**, R[**dY**]L[**Oic**]T-OH: 703.7 (calc. 703.8).

The molecular dynamic simulations study of the proctolin receptor docking model. The structure of proctolin receptor was built by using GPCR I-TASSER (Iterative Threading ASSEMBLY Refinement) server^{32–35}. The C-terminal of proctolin receptor was removed. The homology model of proctolin receptor was used to dock with proctolin. The Induced Fit Docking (IFD) method³⁶ was used to obtain the preliminary results. Then the preliminary results from the IFD were used to dock by QM-Polarized Ligand Docking method. All of the docking process were implemented in Maestro software (Schrodinger Release 2019–3).

We used the previous docking model of proctolin and proctolin receptor to keep the simulation study. CHARMM-GUI was used to embed the docking model of proctolin receptor with proctolin into the 1-palmitoyl-2-oleoyl-sn-glycero-3-phosphocholine (POPC) lipid bilayer environment, and length of X and Y are 80 Å which is perpendicular to the z-direction, the length of Z is 132 Å⁵⁷. The Cl⁻ ions were added to generate a neutral system. Amber17 was used to run the solvated structures by MD simulations and AMBER force field, ff14SB, was applied for the MD simulation protein⁵⁸. The particle mesh Ewald method was used to calculate the long-range electrostatic interactions⁵⁹. First, the system was minimized in 5000 steps while positional restraints for proteins, and ligand, and lipid head groups. The lipid structures were keeping dihedral restraints. Then, the system was equilibrated for 50 ps at 303.15 K (NVT ensemble) and 325 ps (NPT ensemble). The temperature was controlled by using a Langevin thermostat with a friction coefficient 1.0 ps⁻¹, the pressure was controlled by Monte-Carlo barostats. The time step of the simulations was 0.002 ps, the total production time was 1.0 μs. VMD software was used to analyze the MD trajectory. Figures were processed by ChimeraX^{60,61}.

Data availability

The nucleotide sequence was deposited in NCBI GenBank with the accession number MN462557.1.

Received: 20 June 2022; Accepted: 8 September 2022

Published online: 14 October 2022

References

- Anderson, D. L. & Trueman, J. W. H. *Varroa jacobsoni* (Acari: Varroidae) is more than one species. *Exp. Appl. Acarol.* **24**, 165–189 (2000).
- Evans, J. D. & Cook, S. C. Genetics and physiology of *Varroa* mites. *Curr. Opin. Insect Sci.* **26**, 130–135. <https://doi.org/10.1016/j.cois.2018.02.005> (2018).
- Di Prisco, G. et al. *Varroa destructor* is an effective vector of Israeli acute paralysis virus in the honeybee, *Apis mellifera*. *J. Gen. Virol.* **92**, 151–155. <https://doi.org/10.1099/vir.0.023853-0> (2011).

4. Wang, H. *et al.* Sequence recombination and conservation of *Varroa destructor* virus-1 and deformed wing virus in field collected honey bees (*Apis mellifera*). *PLoS One* <https://doi.org/10.1371/journal.pone.0074508> (2013).
5. Haber, A. I., Steinhauer, N. A. & van Engelsdorp, D. Use of chemical and nonchemical methods for the control of *Varroa destructor* (Acari: *Varroidae*) and associated winter colony losses in U.S. beekeeping operations. *J. Econ. Entomol.* **112**, 1509–1525. <https://doi.org/10.1093/jee/toz088> (2019).
6. Weinstock, G. M. *et al.* Insights into social insects from the genome of the honeybee *Apis mellifera*. *Nature* **443**, 931–949. <https://doi.org/10.1038/nature05260> (2006).
7. Hillesheim, E., Ritter, W. & Bassand, D. First data on resistance mechanisms of *Varroa jacobsoni* (OUD) against tau-fluvalinate. *Exp. Appl. Acarol.* **20**, 283–296 (1996).
8. Maggi, M. D., Ruffinengo, S. R., Damiani, N., Sardella, N. H. & Eguaras, M. J. First detection of *Varroa destructor* resistance to coumaphos in Argentina. *Exp. Appl. Acarol.* **47**, 317–320. <https://doi.org/10.1007/s10493-008-9216-0> (2009).
9. Milani, N. The resistance of *Varroa jacobsoni* Oud to pyrethroids: a laboratory assay. *Apidologie* **26**, 415–429 (1995).
10. Milani, N. The resistance of *Varroa jacobsoni* Oud. to acaricides. *Apidologie* **30**, 229–234 (1999).
11. Campbell, E. M., Budge, G. E., Watkins, M. & Bowman, A. S. Transcriptome analysis of the synganglion from the honey bee mite, *Varroa destructor* and RNAi knockdown of neural peptide targets. *Insect Biochem. Molec.* **70**, 116–126. <https://doi.org/10.1016/j.ibmb.2015.12.007> (2016).
12. Leonard, S. P. *et al.* Engineered symbionts activate honey bee immunity and limit pathogens. *Science* **367**, 573–576. <https://doi.org/10.1126/science.aax9039> (2020).
13. Jiang, H. *et al.* Ligand selectivity in tachykinin and natalisin neuropeptidergic systems of the honey bee parasitic mite *Varroa destructor*. *Sci. Rep.-UK* <https://doi.org/10.1038/srep19547> (2016).
14. Veenstra, J. A. Coleoptera genome and transcriptome sequences reveal numerous differences in neuropeptide signaling between species. *PeerJ* <https://doi.org/10.7717/peerj.7144> (2019).
15. Spittaels, K. *et al.* Isolation of Ala(1)-proctolin, the first natural analog of proctolin, from the brain of the Colorado potato beetle. *Mol. Cell Endocrinol.* **110**, 119–124 (1995).
16. Schoville, S. D. *et al.* A model species for agricultural pest genomics: The genome of the Colorado potato beetle, *Leptinotarsa decemlineata* (Coleoptera: Chrysomelidae). *Sci. Rep.* **8**, 1931. <https://doi.org/10.1038/s41598-018-20154-1> (2018).
17. Egerod, K. *et al.* Molecular identification of the first insect proctolin receptor. *Biochem. Biophys. Res. Commun.* **306**, 437–442. [https://doi.org/10.1016/S0006-291x\(03\)00997-5](https://doi.org/10.1016/S0006-291x(03)00997-5) (2003).
18. Johnson, E. C. *et al.* Identification and characterization of a G protein-coupled receptor for the neuropeptide proctolin in *Drosophila melanogaster*. *Proc. Natl. Acad. Sci. USA* **100**, 6198–6203 (2003).
19. Brown, B. E. & Starratt, A. N. Isolation of proctolin, a myotropic peptide, from *Periplaneta americana*. *J. Insect Physiol.* **21**, 1879–1881 (1975).
20. Clark, L., Agricola, H. J. & Lange, A. B. Proctolin-like immunoreactivity in the central and peripheral nervous systems of the locust, *Locusta migratoria*. *Peptides* **27**, 549–558. <https://doi.org/10.1016/j.peptides.2005.06.027> (2006).
21. Gray, A. S., Osborne, R. H. & Jewess, P. J. Pharmacology of proctolin receptors in the isolated foregut of the locust *Schistocerca gregaria* - identification of [Alpha-Methyl-L-Tyrosine(2)]-proctolin as a potent receptor antagonist. *J. Insect Physiol.* **40**, 595–600 (1994).
22. Lange, A. B. & Clark, L. The distribution and physiological effects of proctolin in the locust, *Locusta migratoria*. *Comp. Biochem. Physiol. A* **141**, S106–S106 (2005).
23. Puiroux, J., Pedelaborde, A. & Loughton, B. G. Characterization of a proctolin binding-site on locust hindgut membranes. *Insect Biochem. Molec.* **22**, 547–551 (1992).
24. Walther, C. & Zittlau, K. E. Do YGGFMRFamide and proctolin act on the same potassium conductance in locust skeletal-muscle. *J. Physiol.-London* **410**, P32–P32 (1989).
25. Davis, N. T., Velleman, S. G., Kingan, T. G. & Keshishian, H. Identification and distribution of a proctolin-like neuropeptide in the nervous-system of the gypsy moth, *Lymantria dispar*, and in Other *Lepidoptera*. *J. Comp. Neurol.* **283**, 71–85 (1989).
26. Zittman, D., Kingan, T. G., Kramer, S. J. & Beckage, N. E. Accumulation of neuropeptides in the cerebral neurosecretory system of *Manduca sexta* larvae parasitized by the braconid wasp *Cotesia congregata*. *J. Comp. Neurol.* **356**, 83–100 (1995).
27. Brown, B. E. Occurrence of proctolin in 6 orders of insects. *J. Insect Physiol.* **23**, 861–864 (1977).
28. Fianra, L., Casartelli, M., Diamante, B. & Giordana, B. Proctolin affects gut functions in lepidopteran larvae. *J. Appl. Entomol.* **134**, 745–753. <https://doi.org/10.1111/j.1439-0418.2009.01501.x> (2010).
29. Miranda, C. R. E., Bitondi, M. M. G. & Simoes, Z. L. P. Effect of proctolin on the egg-laying activity of *Apis mellifera* queens. *J. Apicult. Res.* **42**, 35–38 (2003).
30. Park, Y., Kim, Y. J., Dupriez, V. & Adams, M. E. Two subtypes of ecdysis-triggering hormone receptor in *Drosophila melanogaster*. *J. Biol. Chem.* **278**, 17710–17715. <https://doi.org/10.1074/jbc.M301119200> (2003).
31. Jiang, H. B. *et al.* Functional characterization of five different PRXamide receptors of the red flour beetle *Tribolium castaneum* with peptidomimetics and identification of agonists and antagonists. *Peptides* **68**, 246–252. <https://doi.org/10.1016/j.peptides.2014.11.004> (2015).
32. Roy, A., Kucukural, A. & Zhang, Y. I-TASSER: a unified platform for automated protein structure and function prediction. *Nat. Protoc.* **5**, 725–738 (2010).
33. Yang, J. *et al.* The I-TASSER Suite: Protein structure and function prediction. *Nat. Methods* **12**, 7–8 (2015).
34. Yang, J. & Zhang, Y. I-TASSER server: New development for protein structure and function predictions. *Nucleic Acids Res.* **43**, W174–W181 (2015).
35. Zhang, J., Yang, J., Jang, R. & Zhang, Y. GPCR-I-TASSER: A hybrid approach to G protein-coupled receptor structure modeling and the application to the human genome. *Structure* **23**, 1538–1549 (2015).
36. Sherman, W., Day, T., Jacobson, M. P., Friesner, R. A. & Farid, R. Novel procedure for modeling ligand/receptor induced fit effects. *J. Med. Chem.* **49**, 534–553 (2006).
37. Mazzocco, C., Fukasawa, K. M., Raymond, A. A. & Puiroux, J. Purification, partial sequencing and characterization of an insect membrane dipeptidyl aminopeptidase that degrades the insect neuropeptide proctolin. *Eur. J. Biochem.* **268**, 4940–4949 (2001).
38. Gray, A. S. & Osborne, R. H. [Alpha-Methyl-Tyrosine(2)]-proctolin blocks proctolin receptors in the locust foregut. *Brit. J. Pharmacol.* **112**, U66–U66 (1994).
39. Hinton, J. M., Osborne, R. H., Bartosz-Bechowski, H. & Konopinska, D. Myotropic effects of proctolin analogues, modified in position 2 of the peptide chain, on the foregut of the locust *Schistocerca gregaria*. *J. Insect Physiol.* **42**, 449–454 (1996).
40. Hinton, J. M., Osborne, R. H., Odell, B., Hammond, S. J. & Blagbrough, I. S. Cycloproctolin and [alpha-methyl-L-Tyr]-proctolin are potent antagonists of proctolin-induced inositol phosphate production in locust foregut homogenates. *Bioorg. Med. Chem. Lett.* **5**, 3007–3010 (1995).
41. Konopinska, D. Insect neuropeptide proctolin and its analogues - An overview of the present literature. *J. Pept. Res.* **49**, 457–466 (1997).
42. Konopinska, D., Bartosz-Bechowski, H., Rosinski, G. & Sobotka, W. New proctolin analogs modified in position-4 of the peptide-chain and their influence on the heart-beat frequency of insects. *B Pol. Acad. Sci.-Chem.* **41**, 27–39 (1993).
43. Konopinska, D., Rosinski, G., Sobotka, W. & Plech, A. Proctolin and its analogs - structure biological function relationship studies. *Pol. J. Chem.* **68**, 1437–1439 (1994).

44. Mazzocco-Manneval, C. *et al.* Pharmacological studies of proctolin receptors on foregut and hindgut of *Blaberus craniifer*. *Peptides* **19**, 1641–1651 (1998).
45. Woznica, I., Rosinski, G. & Konopinska, D. New proctolin analogues modified in position 2 or 3 of the peptide chain and their myotropic effects in insects. *Pol. J. Chem.* **76**, 1425–1431 (2002).
46. Nachman, R. J. *et al.* Enhanced in vivo activity of peptidase-resistant analogs of the insect kinin neuropeptide family. *Peptides* **23**, 735–745. [https://doi.org/10.1016/S0196-9781\(01\)00654-4](https://doi.org/10.1016/S0196-9781(01)00654-4) (2002).
47. Nachman, R. J., Teal, P. E. A. & Strey, A. Enhanced oral availability/pheromonotropic activity of peptidase-resistant topical amphiphilic analogs of pyrokinin/PBAN insect neuropeptides. *Peptides* **23**, 2035–2043. [https://doi.org/10.1016/S0196-9781\(02\)00191-2](https://doi.org/10.1016/S0196-9781(02)00191-2) (2002).
48. Ding, X. Y., Zhao, X. & Watts, A. G-protein-coupled receptor structure, ligand binding and activation as studied by solid-state NMR spectroscopy. *Biochem. J.* **450**, 443–457. <https://doi.org/10.1042/Bj20121644> (2013).
49. Kobilka, B. Structural insights into the dynamic process of G protein-coupled receptor activation. *Faseb J.* **27** (2013).
50. Kobilka, B. K. G protein coupled receptor structure and activation. *Bba-Biomembranes* **1768**, 794–807. <https://doi.org/10.1016/j.bbame.2006.10.021> (2007).
51. Kumar, S., Stecher, G. & Tamura, K. MEGA7: Molecular evolutionary genetics analysis version 7.0 for bigger datasets. *Mol. Biol. Evol.* **33**, 1870–1874. <https://doi.org/10.1093/molbev/msw054> (2016).
52. Aikins, M. J. *et al.* Vasopressin-like peptide and its receptor function in an indirect diuretic signaling pathway in the red flour beetle. *Insect Biochem. Molec.* **38**, 740–748. <https://doi.org/10.1016/j.ibmb.2008.04.006> (2008).
53. Jiang, H., Wei, Z., Nachman, R. J., Adams, M. E. & Park, Y. Functional phylogenetics reveals contributions of pleiotropic peptide action to ligand-receptor coevolution. *Sci. Rep.* **4**, 6800. <https://doi.org/10.1038/srep06800> (2014).
54. De Smet, L. *et al.* Stress indicator gene expression profiles, colony dynamics and tissue development of honey bees exposed to sub-lethal doses of imidacloprid in laboratory and field experiments. *PLoS ONE* <https://doi.org/10.1371/journal.pone.0171529> (2017).
55. Gui, S. H. *et al.* Assessment of insecticidal effects and selectivity of CAPA-PK peptide analogues against the peach-potato aphid and four beneficial insects following topical exposure. *Pest Manag. Sci.* <https://doi.org/10.1002/ps.5971> (2020).
56. Taneja-Bageshwar, S. *et al.* Biostable agonists that match or exceed activity of native insect kinins on recombinant arthropod GPCRs. *Gen. Comp. Endocr.* **162**, 122–128. <https://doi.org/10.1016/j.yggen.2008.10.013> (2009).
57. Wu, E. L. *et al.* (Wiley Online Library, 2014).
58. Maier, J. A. *et al.* ff14SB: Improving the accuracy of protein side chain and backbone parameters from ff99SB. *J. Chem. Theory Comput.* **11**, 3696–3713 (2015).
59. Petersen, H. G. Accuracy and efficiency of the particle mesh Ewald method. *J. Chem. Phys.* **103**, 3668–3679 (1995).
60. Goddard, T. D. *et al.* UCSF ChimeraX: Meeting modern challenges in visualization and analysis. *Protein Sci.* **27**, 14–25 (2018).
61. Pettersen, E. F. *et al.* UCSF ChimeraX: Structure visualization for researchers, educators, and developers. *Protein Sci.* **30**, 70–82 (2021).

Acknowledgements

This study is contribution No. 23-056-J from the Kansas Agricultural Experiment Station. This research was funded partially by NIH-NIAID R21 AI163423 and USDA-NIFA GRANT13066347 to YP.

Author contributions

The first two authors, V.J. and D.L. contributed equally to this work. G.S., T.A., H.-L.N., R.N., and Y.P. designed research; V.J., D.L., L.R., S.F., R.S., M.M., Y.Z., K.K., J.Z., and S.G. performed research; M.S. analyzed data; G.S., T.A., H.-L.N., R.N., and Y.P. wrote the paper and supervised the research.

Competing interests

The authors declare no competing interests.

Additional information

Supplementary Information The online version contains supplementary material available at <https://doi.org/10.1038/s41598-022-20110-0>.

Correspondence and requests for materials should be addressed to Y.P.

Reprints and permissions information is available at www.nature.com/reprints.

Publisher's note Springer Nature remains neutral with regard to jurisdictional claims in published maps and institutional affiliations.



Open Access This article is licensed under a Creative Commons Attribution 4.0 International License, which permits use, sharing, adaptation, distribution and reproduction in any medium or format, as long as you give appropriate credit to the original author(s) and the source, provide a link to the Creative Commons licence, and indicate if changes were made. The images or other third party material in this article are included in the article's Creative Commons licence, unless indicated otherwise in a credit line to the material. If material is not included in the article's Creative Commons licence and your intended use is not permitted by statutory regulation or exceeds the permitted use, you will need to obtain permission directly from the copyright holder. To view a copy of this licence, visit <http://creativecommons.org/licenses/by/4.0/>.

© The Author(s) 2022